THE JOURNAL OF BIOLOGICAL CHEMISTRY
Vol. 273, No. 52, Issue of December 25, pp. 34992–34999, 1998
Printed in U.S.A.

Structure-Activity of Tetrad-forming Oligonucleotides as a Potent Anti-HIV Therapeutic Drug*

(Received for publication, March 11, 1998, and in revised form, October 5, 1998)

Naijie Jing‡§ and Michael E. Hogan‡¶‖

From the ‡Department of Molecular Physiology and Biophysics, Baylor College of Medicine, Houston, Texas 77030 and ¶Genometrix, Inc., The Woodlands, Texas 77381

Recently, we have described the design and characterization of oligonucleotides containing only G and T bases, *i.e.* T30695 and T30177, that are potent inhibitors of human immunodeficiency virus type 1 (HIV-1) replication in culture (Jing, N., Rando, R. F., Pommier, Y., and Hogan, M. E. (1997) *Biochemistry* 36, 12498–12505). To understand that observation and to rationalize the generally high thermal stability of oligonucleotide folding for these compounds, we have used NMR methods, coupled to molecular modeling, to obtain a high resolution structure model for T30695, which is the most potent of the integrase inhibitors that have been identified thus far. Modeling and NMR data obtained in the presence of Li^+ ions show that T30695 assumes an intramolecular fold with a distorted G-octet core and a set of three open, partially disordered loops. This is referred to as Li^+-form structure. The NMR-based model suggests that, upon coordination with three K^+ equivalents, the central G-octet becomes more regular and that the loop domains become orderly and compact. This is referred to as K^+-form structure. Based upon the assay of inhibition of HIV-1 integrase, T30695 demonstrated a strong inhibition of HIV-1 integrase activity as the K^+-form structure, but a poor inhibition of HIV-1 integrase activity as the Li^+-form structure. The structure/activity analysis suggests that the K^+-induced conformation transition of the tetrad-forming oligonucleotides, such as T30695 and T30177, plays a key role in inhibition of HIV-1 integrase activity.

Integration of HIV-1[1] viral DNA into a host chromosome is an essential step for its replication (1). As the only enzyme required for HIV-1 integration, integrase catalyzes the insertion of HIV-1 viral DNA into the host genome in a two-step reaction. First, integrase cleaves two nucleotides from the 3′-end of the linear proviral DNA. Then, upon binding to the proviral duplex, integrase catalyzes the covalent coupling of the cleaved 3′-end to a site of the host chromosome, which had been nicked by the integrase (1–3). Since it is critical to HIV-1 viral replication, integrase has become an attractive target for selective anti-HIV therapies. Pharmaceutical inhibition of HIV-1 integration has been reported for 3′-azido-3′-deoxythymidine (4), deoxyriboses with substitution or unsaturation at the 3′-position (5), tyrphostins (6), cosalane analogues (7), and triplex-forming oligonucleotides (8). All of the candidates mentioned above had an IC_{50} in the micromolar range for inhibition of the strand transfer or the terminal exonuclease activity, which is too high to be of general utility.

Recently, a new class of oligonucleotides was developed to be an inhibitor of HIV-1 integrase (9). The most potent anti-HIV-1 oligonucleotide in this oligomer family was reported to be a 17-mer (T30177), 5′-g*tggtgggtgggtggg*t, synthesized with two phosphorothioate linkages (one at each end). According to preliminary physical analysis, it was proposed that T30177 formed an intramolecular G-quartet structure (9). Previously, it had been shown that T30177 can inhibit both the activity of HIV-1 integrase with IC_{50} values in the 50 nM range (10).

Based upon T30177, a 16-residue oligonucleotide, T30695, 5′-g*ggtgggtgggtggg*t, was designed in order to improve both the structural stability and the inhibition of HIV-1 integrase activity (11). Thermal denaturation analysis demonstrated that T30695 folded into an extremely stable intramolecular G-quartet structure in the presence of K^+. Compared with T30177, the melting temperature of T30695 was substantially increased. In the presence of K^+, T30695 folded into a stable G-quartet structure as a two-step process as follows: the first being a fast, higher affinity ion binding process, apparently at the central pair of G-quartets; the second being localized to the loop domains to yield two additional lower affinity ion binding sites. Recent NMR results support the two-step binding model: the first step saturating at about a 1:1 ratio of T30695 to K^+, and the second step saturating at about a ratio of 1:3 (12). It was also proposed that K^+ binding to the loop domains of T30695 induced a structural rearrangement, in which loop bases were oriented parallel to the bases of the G-quartet core (Fig. 1). By using a standard gel-based integrase assay, IC_{50} (50% inhibitory concentration) values for inhibition of HIV-1 integrase by T30695 were determined. The values for the 3′-processing and strand transfer steps were 43 and 24 nM, respectively, and about 70 nM for inhibition of HIV-1 proliferation in culture (11). Compared with T30695 with three T-G loops and one T-G pseudo loop at its terminus, a closely related homologue, referred to as thrombin-binding aptamer (TBA), also forms an intramolecular G-quartet structure with two T-T loops and one T-G-T loop (13, 14) (Fig. 1*B*). Based upon previous observations (11), the subtle changes in the loop structure substantially decrease their thermal stability, ion binding interaction, and anti-HIV-1 activity.

In order to explore the effect of loop structure on structure and activity, in the present report we have calculated an NMR-derived molecular structure for T30695 in the absence and presence of K^+ and measured K^+-induced folding kinetics of T30695, T30177, and TBA. IC_{50} values for the anti-HIV-1 in-

* This work was supported by National Institutes of Health Training Grants USPH T32-HL07676 (to N. J.) and R01 AI32894 (to M. E. H.). The costs of publication of this article were defrayed in part by the payment of page charges. This article must therefore be hereby marked "*advertisement*" in accordance with 18 U.S.C. Section 1734 solely to indicate this fact.

§ To whom reprint requests should be addressed.
‖ To whom correspondence should be addressed. Tel.: 713-798-5729; Fax: 713-798-6033; E-mail: mhogan@bcm.tmc.edu; njing@bcm.tmc.edu.

[1] The abbreviations used are: HIV-1, human immunodeficiency virus type 1; SPA, scintillation proximity assay; NOE, nuclear Overhauser effect; MD, Molecular Dynamics; TBA, thrombin-binding aptamer; r.m.s.d., root mean square deviation.

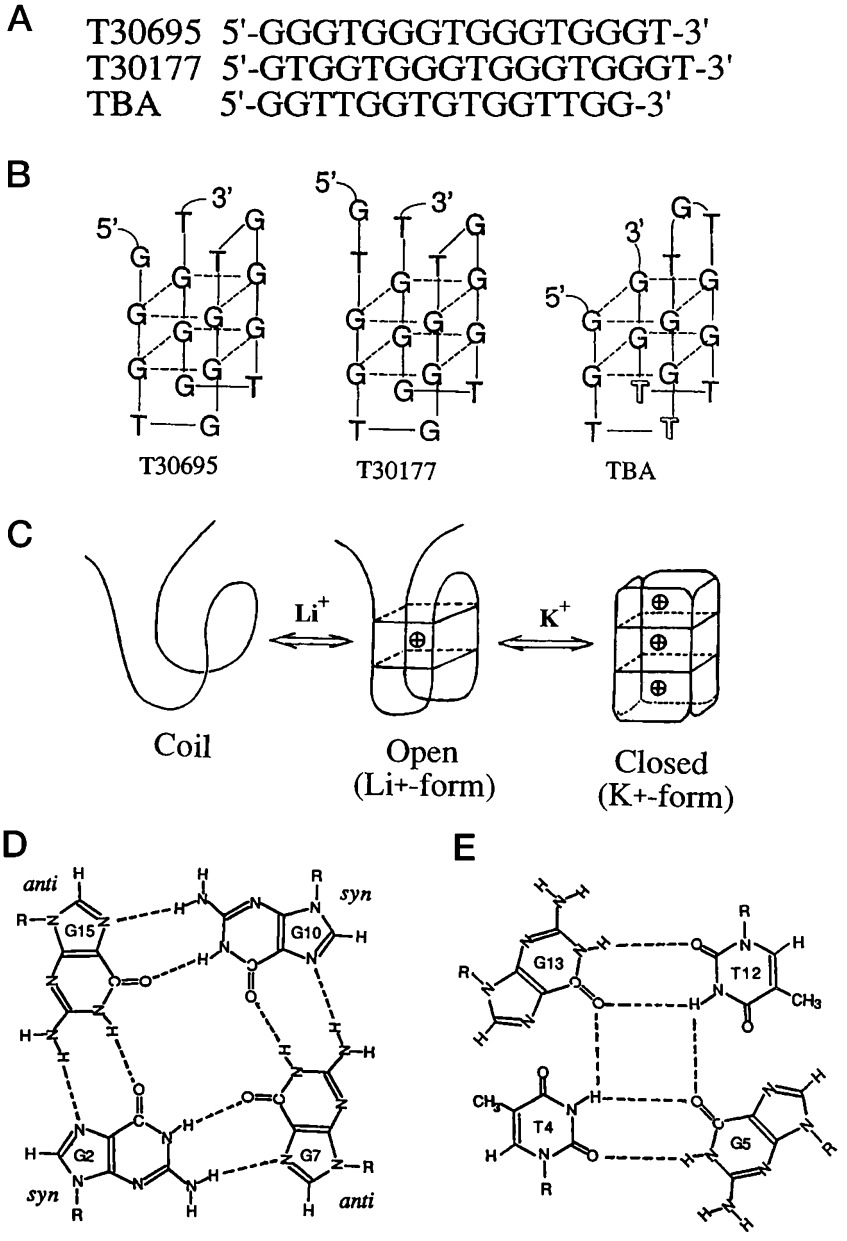

FIG. 1. *A,* sequences of T30695, T30177, and TBA. *B,* anti-parallel G-tetrad folding model and the base numbering formalism for T30695, T30177, and TBA. The formation of G-quartets is indicated by *dashed lines*. *C,* schematic representation of the folding model for T30695 in the absence and the presence of K^+. *D,* the G-quartet, represented by the bases of the G2, G7, G10, and G15 residues, in alternating *syn-* and *anti*-conformations. Hydrogen bonds are in *dashed lines*. *E,* the t-g-t-g-loop base alignment formed in T30695 in the presence of K^+ ions as calculated from NMR and modeling. Hypothetical hydrogen bonds between T O-4 and G imino protons and bifurcated hydrogen bonds, involving G O-6 and T imino protons, are indicated by *dashed lines*.

tegrase activities of T30695, T30177, and TBA were obtained in open and closed structure states (Fig. 1*C*), and the tests were performed commercially at the Southern Research Institute. Based upon the IC_{50} values of T30695, T30177, and TBA in the different structure states, it has been concluded that the K^+-induced conformational transition mediated by orderly folding of the loops of T30695 and T30177 plays a key role in inhibition of HIV-1 integrase activity.

EXPERIMENTAL PROCEDURES

Oligonucleotide Synthesis—Oligonucleotides used in this study were synthesized, purified, and characterized using procedures described previously (9, 11).

NMR Spectroscopy—^{1}H NMR spectra were obtained on an AMX-II 600 MHZ spectrometer (Bruker Instruments, Inc.). Two-dimensional NOESY spectra of T30695 in 20 mM Li_3PO_4, pH 7, with and without K^+ in D_2O and in H_2O were acquired at mixing times of 50, 100, 200,and 350 ms at 22 °C. The jump and return sequence (15) and gradient-tailored water suppression (16) were used in NOESY of T30695 in H_2O. 512 t_1 increments were collected with 64 transients and 2048 complex points for each increment. Homonuclear Hartman-Hahn experiments were conducted with a mixing time of 80 ms using MLEV17 (17). ^{31}P–^{1}H COSY spectra were obtained as described previously (18) with a spectral width of 80 ppm for ^{31}P and 4 ppm for ^{1}H. NMR data were processed using the UXNMR (Bruker) or the FELIX program (Molecular Simulations Inc.) on an INDIGO/ELAN workstation.

Resonance Assignments—^{1}H resonance assignments were made using a combination of through-bond (Phase-sensitive COSY, Homonuclear Hartman-Hahn, ^{1}H–^{31}P COSY) and through-space (NOESY) NMR experiments. Assignments of the deoxyribose spin system were obtained from analysis of COSY and Homonuclear Hartman-Hahn spectra using standard methods (19). Non-exchangeable proton resonances were identified in NOESY in D_2O and the exchangeable resonances were assigned by model-independent quartet assignment. These resonances were used when interpreting through-space connectivity to find assignments (20). Sequence-specific assignments of non-exchangeable resonances were obtained by analyses of NOESY spectra and ^{1}H–^{31}P COSY. Detailed NMR resonance assignments of T30695 have been described elsewhere (12).

Distance Constraints—Proton distance constraints for the structure calculations were obtained from NOESY spectra of T30695 in H_2O and in D_2O collected with mixing times of 50, 100, 200, and 350 ms employing standard methodology (19). The integrated intensity of the most intense H2′–H2″ cross-peaks (I_o) was used for distance calibration and set to 1.9 Å (r_o). The intensities of all other cross-peaks were converted to distances using the $I = I_o(r_{ij}/r_o)^{-6}$ relation, where I is peak integral and r_{ij} is distance between i and j protons. The cross-peak intensities

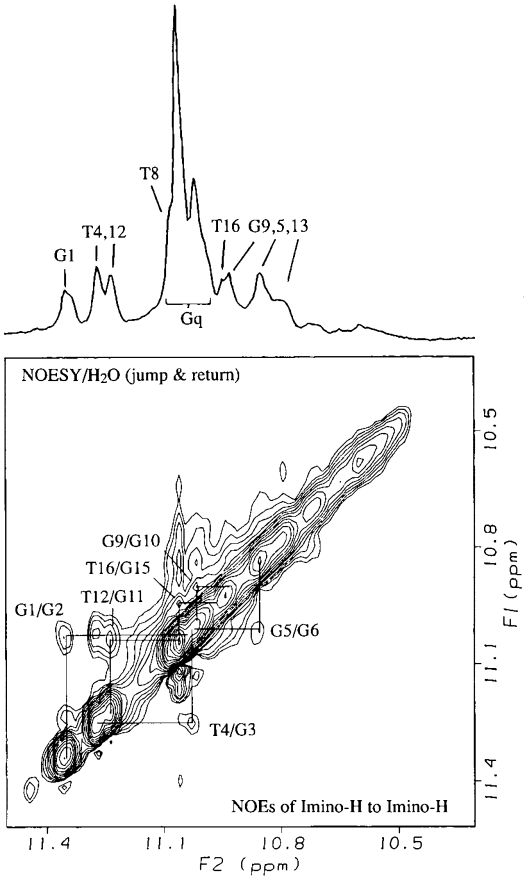

FIG. 2. **NOESY (τ_m = 200 ms) spectrum of T30695 in 10 mM KCl and H_2O (90%), D_2O (10%) using jump and return water suppression.** Data are presented for the exchangeable protons in the H-bonding domain of the NOESY spectrum. NOEs between loop T imino and G_q imino protons, T_mH1-G_{m-1}H1 (m = 4, 8, 12, 16), and between loop G imino and G_q imino protons G_nH1-G_{n+1}H1 (n = 1, 5, 9, 13) were only observed in the presence of K^+ ions, all of which gives significant evidence for the K^+-induced loop folding.

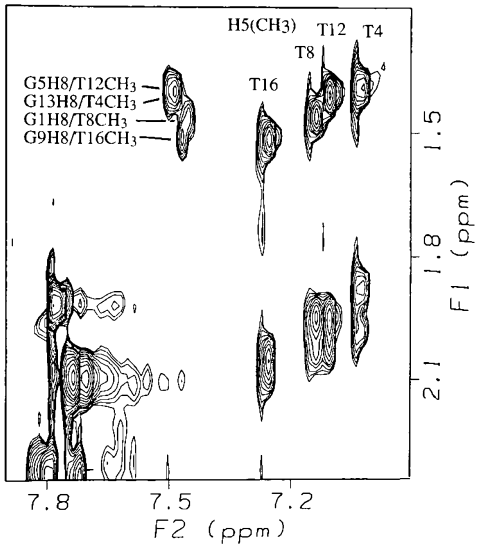

FIG. 3. **The NOESY (τ_m = 200 ms) spectrum of T30695 between loop residues from T methyl to G H8 protons observed in the presence of K^+ ions.** These NOEs serve to establish the orientation of the loop folding.

from the NMR spectra were classified as strong, medium, and weak and were converted to distances with upper limits of 3.0, 4.5, and 5.5 Å, respectively. Based upon a NOESY/H_2O spectrum collected at a mixing time of 200 ms, the distances associated with the cross-peaks were

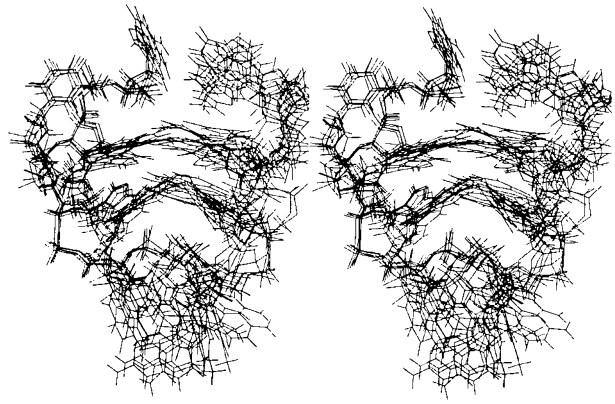

FIG. 4. **A superimposed stereo view of five refined structures of T30695 in the absence of K^+ (Li^+-form structure).** As explained under "Discussion," this structure is an asymmetric, apparently unstable G-quartet with twisted G-quartet plates and opened loops.

estimated to be 2.5, 3.5 and 4.5 (±1.0) Å and were categorized as strong, medium, and weak. The hydrogen bond constraints for the two G-quartets with ideal H-bonding geometry were included in the structure calculation (14). By analogy with the crystallographic structure for G-quartets, a distance of 2.85 (±0.1) Å was assigned for the separation between heavy atoms, and 1.9 (±0.1) Å was assigned for the separation between hydrogen and heavy atoms in the G-quartet H-bonds.

Structure Calculation—By using the distance constraints, calculation of the molecular structure of T30695 was performed in two steps using the DGII (distance geometry) functions of INSIGHTII (Biosym Technologies, San Diego) and the MD (Molecular Dynamics) functions of DISCOVER (Biosym Technologies, San Diego) with the Amber force field on a Silicon Graphics Indigo workstation. An initial quartet structure was created by modification of G-quartet coordinates of the thrombin-binding DNA aptamer from the Protein Data Bank (14). A final structure model was then calculated by the DGII program of INSIGHTII using the following: (i) bound smoothing, in which the triangle and tetrangle inequality bounds were smoothed by Floyd's shortest-paths algorithm; (ii) embedding, which included the selection of a matrix of random trial distances and generation of Cartesian coordinates from trial distances to a distance matrix; and (iii) optimization, which was achieved by minimization of simulated annealing and of conjugate gradients of the error function. The optimization step was reiterated several times until a set of structures had converged into a final group.

Refinement of the DG-calculated structures was carried out by a restrained MD calculation using DISCOVER. The protocol consisted of the following steps: 1) 1000 steps of conjugate gradient energy minimization with a cut-off distance of 6 Å; 2) 30 ps of restrained MD equilibration at 300 K; 3) 100 ps of restrained MD equilibration at 300 K; 4) 1000 steps of conjugate gradient energy minimization with a cut-off distance of 6 Å; and 5) 3000 steps of conjugate gradient energy minimization with a cut-off distance of 12 Å. An apparent force constant of 30 kcal/mol/Å^2 was used for distance restraint.

Assays for Inhibition of HIV-1 Integrase Activity—Anti-integrase activity was carried out in a 96-well based HIV-1 scintillation proximity assay (SPA) by Southern Research Institute, Microbiology Department, Frederick, MD. Methods employed were as described by the manufacturer (Amersham Pharmacia Biotech). Briefly, each test well received 80 μl of premixed solution containing the tritiated oligonucleotide substrates as follows: 10 μl [^{3}H], 50 μl of dithiothreitol (2.8 mg/ml), 20 μl $MgCl_2$, and 10 μl of 10× diluted test compound. Integrase enzyme working solution was prepared in enzyme dilution buffer (20 mM HEPES, pH 7.5, 10 mM dithiothreitol, 0.05%(w/v) Nonidet P-40, and 0.05% (w/v) sodium azide) at a final concentration of 50 nM and then kept on ice. After 10 μl of diluted integrase enzyme was added to each well, the plate was sealed and incubated at 30–33 °C for 1 h. The reaction was terminated by the addition of 10 μl of stop reagent in each well. Then 110 μl of SPA bead solution (100 μl of streptavidin SPA bead suspension and 10 μl of denaturing reagent) was added into each well. The plate was then sealed, mixed by shaking, and incubated at room temperature for 30 min. The reaction in the wells was read on a Wallac MicroBeta Scintillation Counter. The data then were transferred to a spreadsheet embedded with software for calculating the IC_{50} for each test compound.

UV Kinetic Measurements—UV measurements were obtained on an HP 8452A diode array spectrophotometer using an HP 89090A temper-

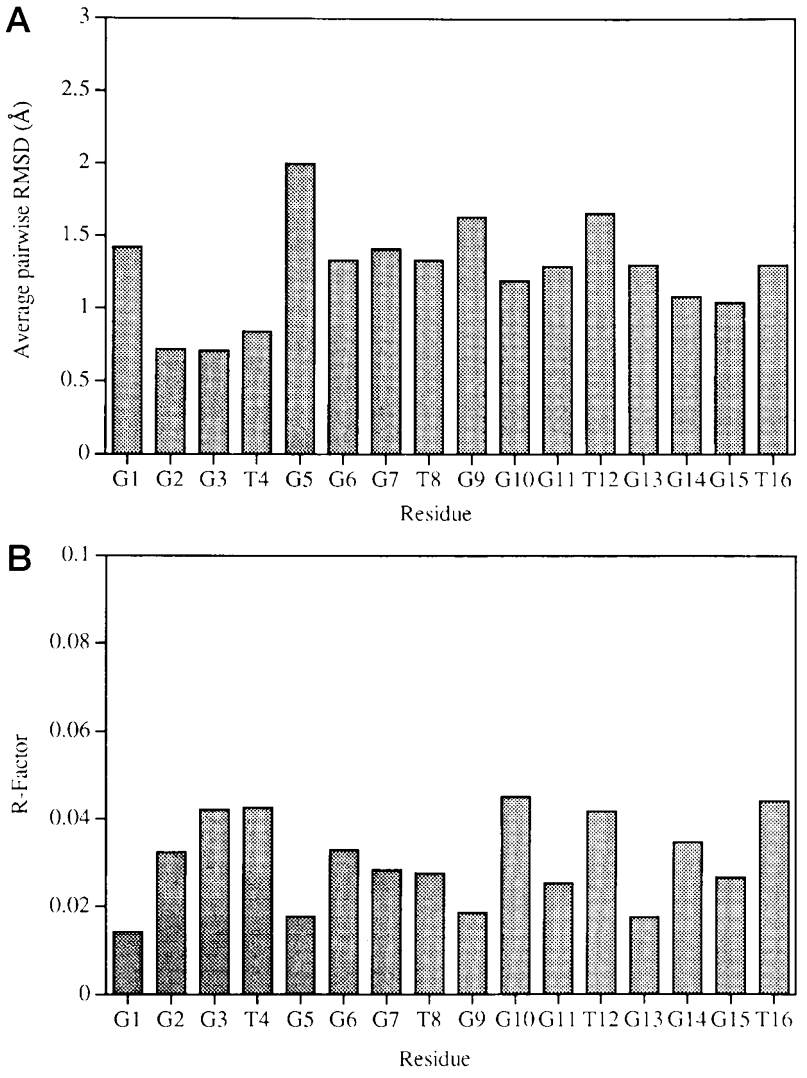

FIG. 5. *A,* r.m.s.d. values per residue with respect to the average coordinates of a best-fit superposition for T30695 in the absence of K^+. *B,* graph of *R*-factor per residue for the refined structure of T30695 in the absence of K^+, calculated from the comparison of the experimental constraints and theoretical calculation (see text for details).

ature regulator. Folding kinetics were obtained by the manual addition of metal ion at $t = 0$, followed by absorption measurement at 264 nm. Mixing dead time was about 5 s. Kinetics were monitored between 10 s and 15 min at 25 °C. The folding time constants, τ, were estimated by fitting the UV kinetic curves using the function of a sum of two exponentials, *i.e.* $A(t) = A_o(\exp(-t/\tau_2) - f\exp(-t/\tau_1))$.

RESULTS

Based on solution state NMR, we have obtained a structural model for T30695 in the absence and presence of K^+ ions. This study is a direct extension of one- and two-dimensional NMR measurements described previously (12). The assignments of non-exchangeable proton resonances and exchangeable proton resonances for T30695 were obtained from NOESY and ^1H–^{31}P COSY. In previous studies, we demonstrated that in the presence of Li^+ ions, T30695 forms an unimolecular tetrad structure stabilized by a pair of G-quartets. Upon addition of K^+ ions up to 3 equivalents, K^+ ions were found to coordinate tightly with T30695 and to induce a second conformational transition (Fig. 1*C*) (12). We also provided preliminary NMR data to suggest that the K^+ binding induced folding of the loop bases onto the planar face of the underlying G-quartets. In the present study, we have calculated NOE distance constraints from the NMR data, and we have used the NOE constraints to obtain a higher resolution structural model for T30695 in the absence of K^+ ion (open form) and in the presence of K^+ ion (the closed form of the intramolecular fold).

NMR Constraints—For NOESY measurements with T30695 in the absence of K^+, 346 NOE cross-peaks were observed, including 37 inter-residue NOEs. The NOE cross-peaks between base H8 and H1′ protons play a key role in the determination of G-quartet structure since they can be used to establish χ angles for the bases. Strong H8–H1′ NOEs were observed for residues G2, G6, G10, and G14, from which we conclude that they assume the *syn*-conformation in the central G-octet (20). Weak NOE peaks between G2H8-G3H1′, G6H8-G7H1′, G10H8-G11H1′, and G14H8-G15H1′ and medium NOEs between G11H8-G10H1′ and G15H8-G14H1′ are consistent with an anti-conformation for those bases. Thus, in the absence of K^+, T30695 appears to assume a standard alternating *syn-anti-syn-anti* G-quartet conformation. This conformation has been observed for other intra- and inter-molecular G-quartets, most notably the analogous intra-molecular G-quartet that has been studied by Feigon and colleagues (20). According to the NOE-based analysis of G-quartet structure (20), the NOEs observed between G_nH8 and G_nH2′, H2″ (for all 8 G residues in the G-quartets) also match the *syn-anti-syn-anti* G-quartet structure for the central core.

96 NOEs (27%) have been assigned to the 8-loop residues of the T30695 fold. The 11 weak inter-residue NOE connections in the loops, T4H6-G13H1′, T12H6-G13H1′, T8H6-G1H1′, and T_nH6-G_{n+1}H2′, H2″ (n = 4, 8, 12, 16), have been used in modeling to constrain the orientation of the loop residues of T30695 in the absence of K^+ ions.

After adding K^+ to T30695 in 20 mM Li_3PO_4, a conforma-

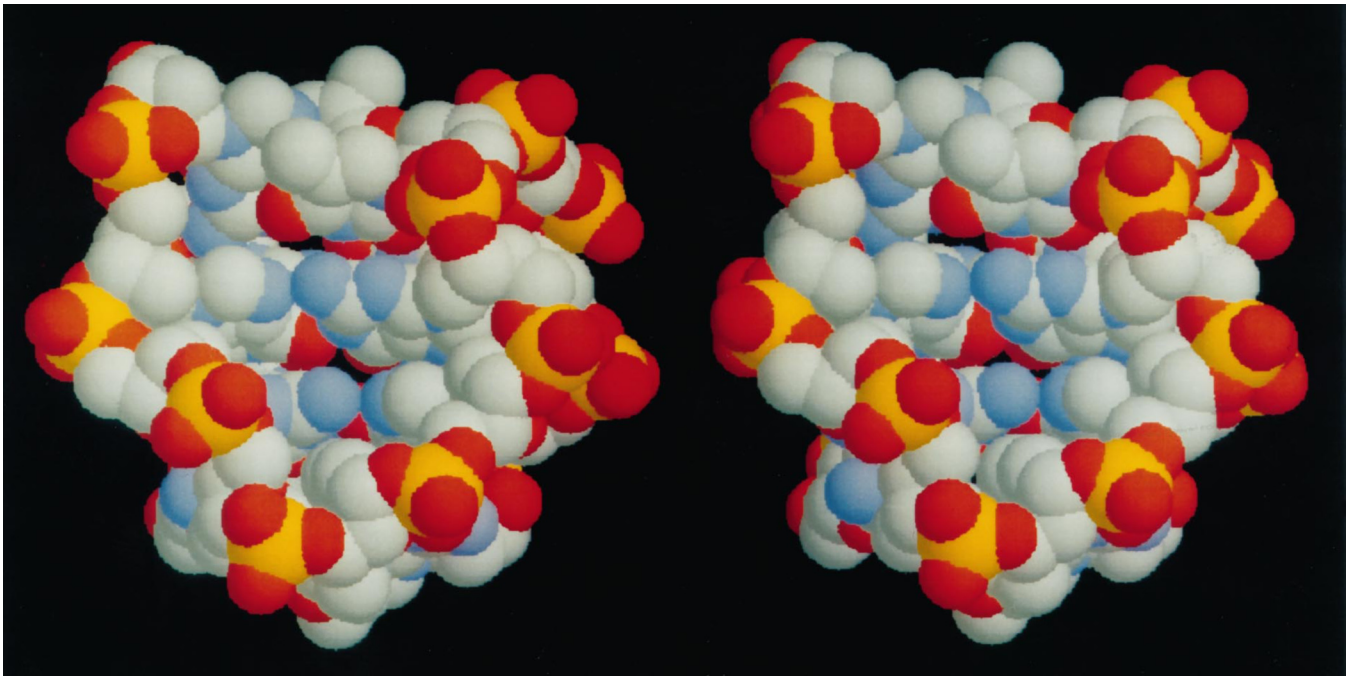

FIG. 6. **The molecular structure of T30695 in the presence of K^+ (K^+-form structure).**

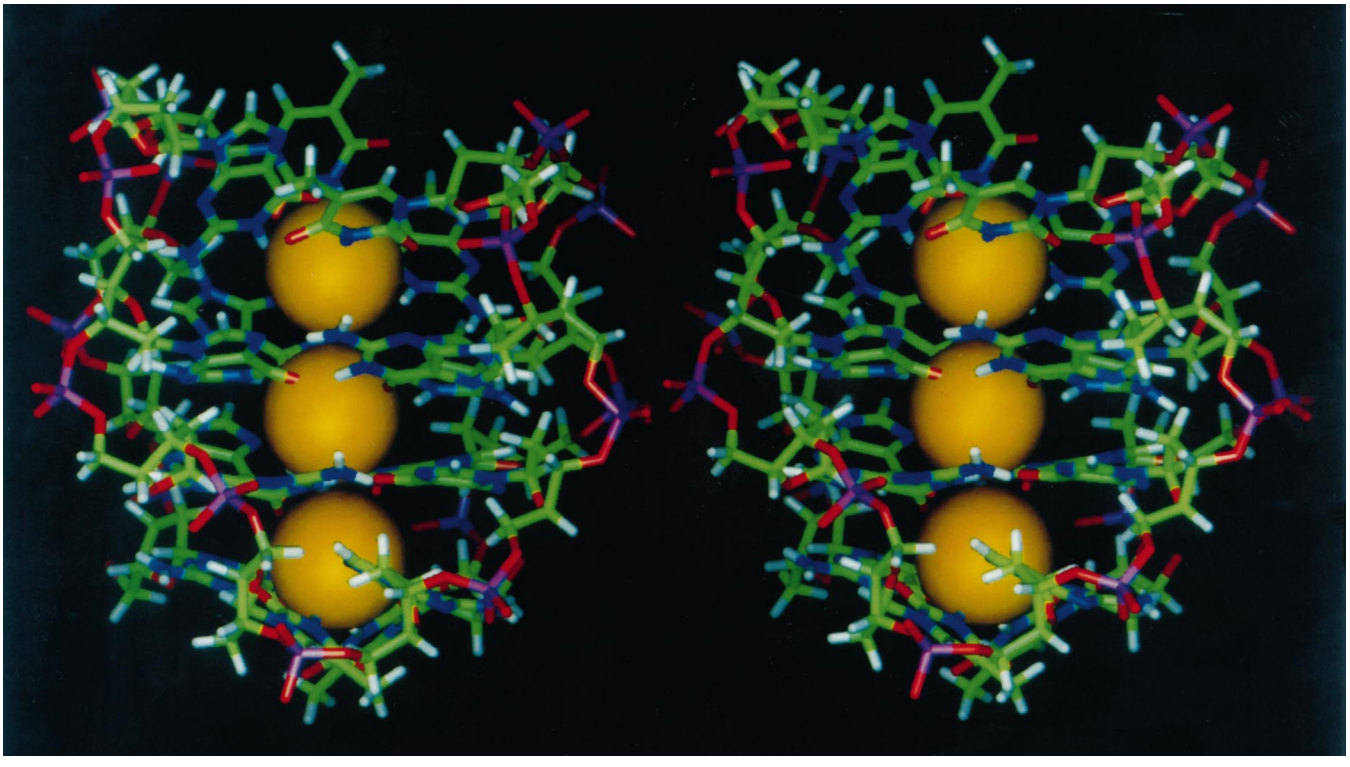

FIG. 7. **The molecular structure of T30695 in the presence of K^+ (K^+-form structure) displaying the position of the three bound K^+ equivalents (see text for details).**

tional transition can be detected by NMR in the loop domains (Fig. 2 and Ref. 12). Sixteen new NOE cross-peaks of the amino and imino protons were observed between a loop and neighboring quartet residues. These cross-peaks were not found in the spectra without K^+. This suggests that in the absence of K^+, the loop residues are open and more dynamic; the separation of the imino and amino protons between a loop and neighbor quartet residues is greater than the maximum NOE-detectable distance. As seen in Fig. 2, the NOE peaks of the imino protons, G_nH1-$G_{n+1}H1$ (n = 1, 5, 9, 13), and T_mH1-$G_{m-1}H1$ (m = 4, 8, 12, 16), provide evidence that the bases of the loop residues, upon binding K^+, fold into an alignment that is parallel to the G-quartet bases. In the presence of K^+ ions, new NOEs between T methyl and G H8 protons were also observed in loop residues in the spectra of T30695 (Fig. 3). These additional constraints suggest a nearly planar fold for the loops (Fig. 1*E*). Comparison of the NOESY spectrum of T30695 in the presence of K^+ with that in the absence of K^+ suggests that the G-quartet and backbone conformation remains unchanged upon binding the 3 eq of the K^+ ion (Ref. 12 and data not shown).

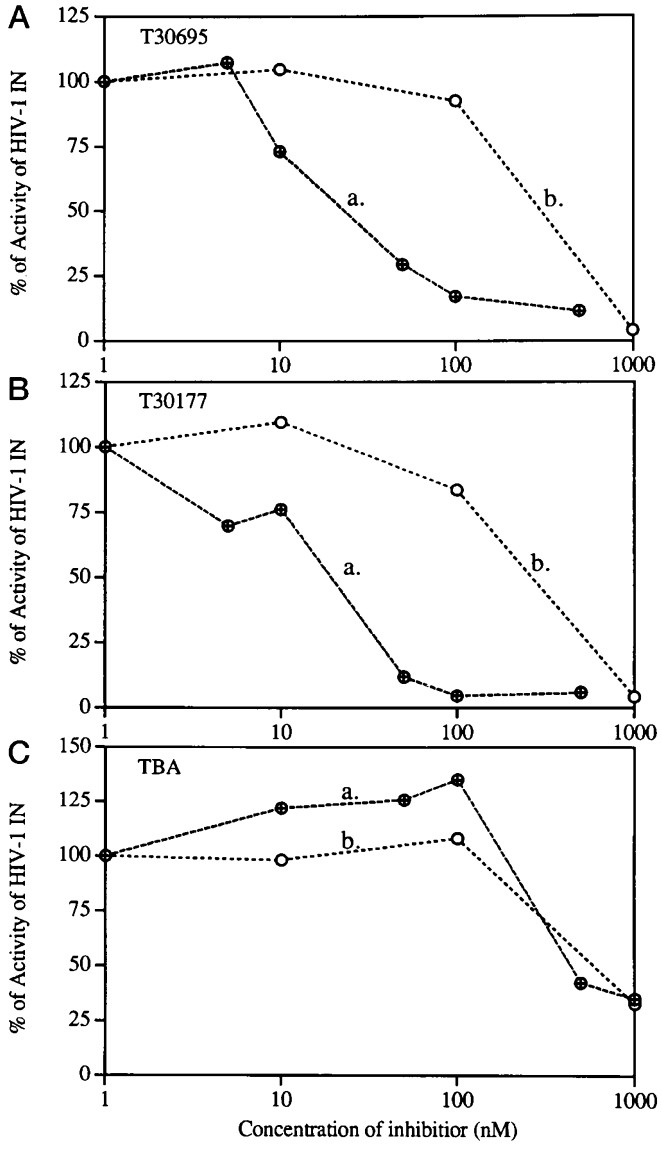

FIG. 8. **The IC_{50} values of T30695 (*A*), T30177 (*B*), and TBA (*C*) obtained from the SPA anti-HIV assay were presented as percentage of activity of HIV-1 integrase *versus* concentration of these oligomers.** Each oligomer was tested in two sample conditions as follows: 1) oligomer in 20 mM Li_3PO_4 in 10 mM KCl (*line a*), and 2) oligomer in 20 mM Li_3PO_4 in H_2O (*line b*), by the same assay process. IC_{50} values of T30695, T30177, and TBA in 10 mM KCl are 31, 26, and 470 nM, and IC_{50} values of T30695, T30177, and TBA in H_2O are 530, 480, and 790 nM, respectively.

TABLE I
The inhibition of HIV-1 integrase activity

Oligomers	5′-Sequence-3′	IC_{50} (nM) 10 mM KCl	IC_{50} (nM) H_2O (with Li^+
T30695	GGGTGGGTGGGTGGGT	31	530
T30177	GTGGTGGGTGGGTGGGT	26	480
TBA	GGTTGGTGTGGTTGG	470	790

Upon binding K^+ ions, the formation of imino proton H bonds between loop T and G residues (Fig. 1*E*) is supported by the large increase in the T_1 relaxation times and downfield chemical shifts for exchangeable loop protons (12). The longer T_1 values may result from residues in a more rigid orientation, which are constrained by hydrogen binding, base-base stacking, and K^+ ion concentration. These additional H bond constraints were included in the calculation of the molecular structure of T30695 in the presence of K^+ ions.

Molecular Structure—Using the NOE distance and H bond constraints, a calculation of the structure of T30695 in the absence and in the presence of K^+ ions was performed by DGII and MD programs using the Amber force field. The details of the protocol for processing NOE data and the calculation of the molecular structures are described under "Experimental Procedures." Fig. 4 shows stereo views of superimposed structures obtained in the refinement of the T30695 structure in the absence of K^+ (Li^+ form, Fig. 1*C*). This family of equivalent structure models reveals a pair of distended G-quartets in the central core flanked by unfolded loops. Convergence was verified by examining the constraint energy and violation list. As seen in Fig. 5*A*, the plot of r.m.s.d. (root mean square deviation) for this structure set shows a reasonable convergence for the G-quartets and a larger deviation for the loop residues. The average r.m.s.d. values of the residues in the pair of G-quartets and in the loops are 1.09 ± 0.28 and 1.44 ± 0.56 Å, respectively. Therefore, the positions of the bases within the G-quartets are well determined. However, the bases of the loop residues appear to be more variable (in the absence of K^+ ions), matching a suggestion made previously (11, 12). The *R*-factor per residue for the refined structure of T30695 in the absence of K^+ was calculated by Equation 1.

$$R = [\Sigma(AX6 - AT6)^2]^{1/2}/\Sigma(AX6), \qquad \text{(Eq. 1)}$$

where $AX6 = |A^{exp}|^{1/6}$ and $AT6 = |A^{theo}|^{1/6}$. The value of the *R*-factor per residue is about 0.028 ± 0.014 as shown in Fig. 5*B*.

Adding the NOE distance constraints obtained in the presence of K^+ into the restraint file, the molecular structure for the K^+ form of T30695 was constructed and refined using restrained MD calculation. After binding three K^+ ions, the structure of T30695 is composed of a central-most pair of G-quartets, and the loop bases are aligned so that they lie roughly parallel to the G-quartet bases (Fig. 6 and 7). This structure is more compact and symmetrical than the structure of T30695 in the absence of K^+. The distance between the two central G-quartet planes is calculated to be 3.9 ± 0.2 Å, which is in agreement with values seen for G-quartet in crystals (21). The average distance of the bases between the residues of G_n to $T_{,+3}$ (n = 1, 5, 9, 13) is approximately 13–15 Å. Since the loops of T30695 fold into symmetrical and nearly identical positions, the width of two ends of the octet is about the same in this calculated structure and is approximately 14–16 Å apart. The bases of the t-g loop domains fold into an irregular planar configuration at the top and bottom of the pair of G-quartets and are calculated to be in direct coordination with two additional K^+ ions. Each of the T methyl groups is pointed out of the folded plane, which is required by the measured NOEs between T methyl and G H8 protons of the loop residues (Fig. 1*E*). The convergence of a set of molecular structures of T30695 in the presence of K^+ ions becomes more homogeneous. The average r.m.s.d. values of the residues in the pair of G-quartets and in the loops are 0.71 ± 0.18 and 0.87 ± 0.29 Å, respectively.

Inhibition of HIV-1 Integrase—Previous work has shown that T30695 and T30177 are both potent HIV-1 inhibitors, but TBA has a poor ability to inhibit HIV-1 integrase (11). In a gel-based assay, IC_{50} values of T30695, T30177, and TBA reported by our collaborators (11) are about 43, 79, and 870 nM for inhibition of HIV-1 integrase 3′-processing and about 24, 49, and 750 nM for inhibition of HIV-1 integrase strand-transfer, respectively. Here we measured IC_{50} values of T30695, T30177, and TBA in two different sample conditions as follows: (i) the oligomers in 20 mM Li_3PO_4, pH 7, were prepared in 10 mM KCl, then diluted into 1 mM KCl as a test concentration, and (ii) the oligomers in 20 mM Li_3PO_4, pH 7, were prepared in H_2O and test IC_{50} values without adding KCl. The measurements of the

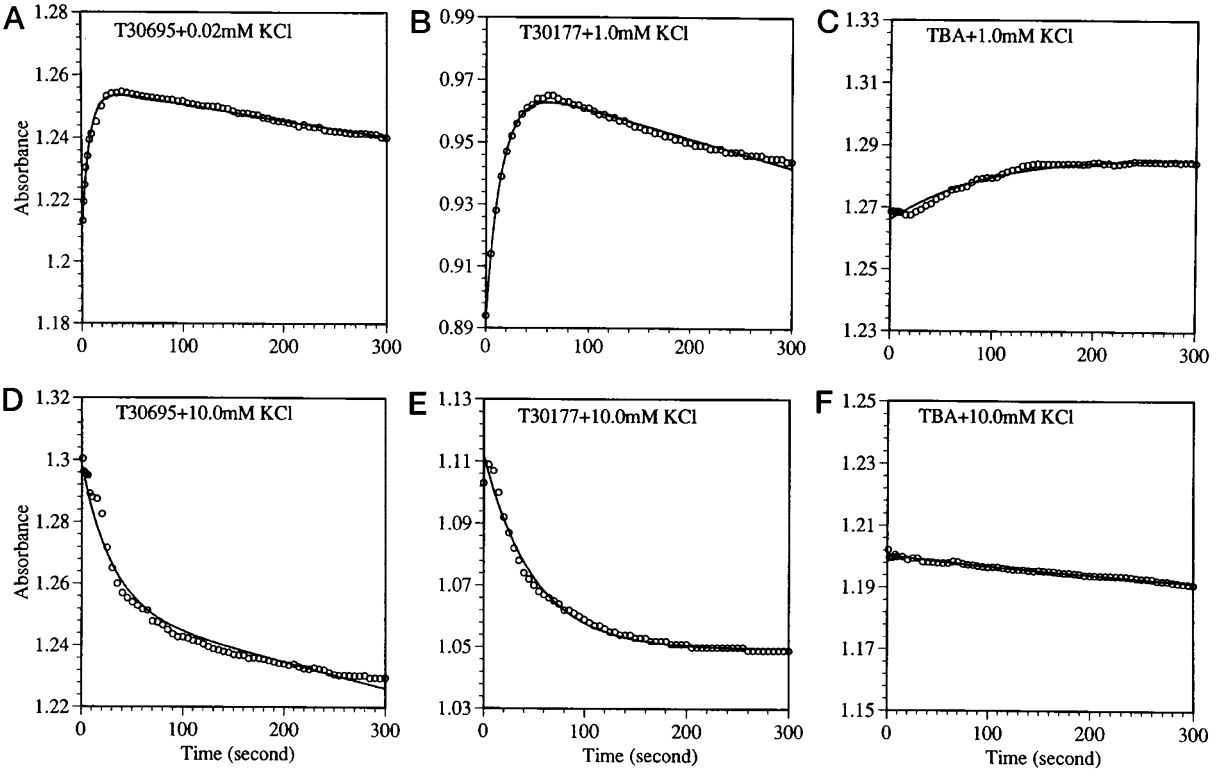

FIG. 9. **K^+ ions were added to oligomers in 20 mM Li_3PO_4 assay buffer at time 0.** Plots were presented by absorbance *versus* time after addition of K^+ ions. Kinetics were measured at added KCl concentrations for T30695: 0.02 mM (*A*) and 10.0 mM (*D*), at added KCl concentrations for T30177; 1.0 mM (*B*) and 10.0 mM (*E*), and added KCl concentration for TBA; 1.0 mM (*C*) and 10.0 mM (*E*). The data have been fitted by a sum of two exponentials: $A\ (t) = A_o\ [\exp(-t/\tau_2) - f\cdot\exp(-t/\tau_1)]$, and the folding time constants, τ_1 and τ_2, were obtained from these curve fittings.

IC_{50} values of T30695, T30177, and TBA with and without K^+ in the final reaction buffer were carried out in the same assay process, which was performed commercially by Southern Research Institute.

As seen in Fig. 8, we found that 50% inhibition of HIV-1 integrase activity by T30695 delivered in a buffer without K^+ corresponds to about 530 nM strand concentration (Fig. 8*A, line b*). The inhibition by T30695 delivered in 10 mM KCl is about 31 nM strand concentration (Fig. 8*A, line a*), 17 times lower than the data obtained in the absence of K^+ ion. The same phenomenon was also observed for T30177 (Fig. 8*B, lines a* and *b*). The IC_{50} value of T30177 delivered in 10 mM KCl is about 18 times lower than that in H_2O (Table I). However, IC_{50} values of TBA with and without K^+ are found to be similar as 470 and 790 nM, respectively (Fig. 8*C, lines a* and *b*), in agreement with a generally K^+-independent aptamer folder (14). As demonstrated above, T30695 forms different molecular structures (K^+ form and Li^+ form) in the presence and absence of K^+ (Figs. 4 and 7). Thus the data in Fig. 8 suggest that the two structures differ greatly in the ability to inhibit HIV-1 integrase.

Kinetics of K^+-induced Structural Transition—In order to further investigate the relation between molecular structure and anti-HIV activity, we measured the kinetics of oligomer folding for T30695, T30177, and TBA using 7 μM strand concentration in 20 mM Li_3PO_4 buffer at 25 °C. Folding kinetics were obtained by manual addition of K^+ at time 0 and measured with UV absorbance at 264 nm in the 0–300-s time range. Since the plots of UV absorption *versus* time for T30695 and T30177 showed a two-step process (Fig. 9, *A* and *B*), the data were analyzed by a simple two-step transitional model: $A\ (t) = A_o[\exp(-t/\tau_2) - f\cdot\exp(-t/\tau_1)]$, where $A_o = C\epsilon l$, C is total concentration of oligomer, ϵ is the extinction coefficient of oligomer sequence, l is path length, and f is fitting constant.

After adding K^+ ions in T30695 and T30177 to 0.02 and 1.0 mM, respectively, the intensity of the UV absorption was found to vary with time. As seen in Fig. 9, *A* and *B*, the folding process as a function of time has two components. The time constant of the first component (τ_1) of T30695 is 8.0 s and that of T30177 is 20.2 s. This component is fast and hyperchromic, and based upon conclusions drawn previously from NMR-based titration (12), it is induced by a K^+ ion competing with a Li^+ ion for binding between the two G-quartets. It appears that in this step, the bases of the two central G-quartets are rearranged into two more regular parallel plates. The second component (τ_2) is slow and hypochromic, indicating a net increase in base stacking, consistent with NMR data that suggests that the loop bases become folded parallel to the bases of the underlying G-quartet by binding two additional K^+ between the loops and G-quartets (12) (Fig. 7). When K^+ was increased to 10 mM, τ_1 was almost too fast to be detected by the apparatus, and τ_2 becomes much faster (Fig. 9, *D* and *E*). τ_2 of T30695 decreased from 2.4×10^4 s (Fig. 9*A*) to 30 s (Fig. 9*D*) and of T30177 decreased from 2.4×10^4 s (Fig. 9*B*) to 50 s (Fig. 9*E*). Thus, the overall folding process of T30695 and T30177 is mainly determined by the time constant (τ_2) of second component, loop rearrangement. The folding process of TBA in 1.0 mM KCl was observed to be a one-step process (τ_1 = 101 s) (Fig. 9*C*). When K^+ concentration was increased to 10 mM, the first step becomes too fast to detect, and no second step was observed (Fig. 9, *C* and *F*). It is clear that there is only one step in the K^+-driven folding process for TBA since only one K^+ is bound into the G-quartet of TBA.

DISCUSSION

In an earlier study (9) we provided evidence to suggest that the 17-mer oligonucleotide T30177 folded intramolecularly to form a structure stabilized by a pair of G-quartets (Fig. 1). We previously noticed that the T30177 fold is significantly more

stable with respect to thermal denaturation (9) than the folded structure of a closely related oligonucleotide, the so-called thrombin binding aptamer (TBA), which had also been shown to form an intramolecular fold stabilized by a single pair of G-tetrads (13, 14). To explain that striking difference (the T_m for T30177 is about 30 ° higher), we proposed that the loop domains of T30177 bind with metal ions, especially K^+, to yield two additional quartet-like base pairings within the loops (Fig. 1*C*). Based upon that low resolution model, we had concluded that the quality of those additional loop interactions and, consequently, the thermodynamic stability of the fold might be additionally improved by elimination of a single base to yield the 16-mer T30695 (11). That predicted stability increase was shown to be correct, which conferred general credibility to the low resolution structural model (11).

One interesting aspect of the folding model for T30177 and T30695 is that the folded state is obtained as a result of a multi-state process (Fig. 1*C*). Based upon ion titration and kinetic studies, we proposed that folding could be adequately modeled as a two-step process. The first step is a transition from a random coil to an extended intramolecular G-tetrad; the second step is compaction of the G-tetrad that results from flattening and stiffening of the loop domains due to K^+ ion binding (11, 12).

Based upon the ion dependence of the folding kinetics (Ref. 11 and Fig. 9) and the ion dependence of ^{1}H NMR parameters (12), we have shown that the first step in the process involves coordination of a single metal ion equivalent to the central pair of G-quartets. The second folding step (namely ordering and compaction of the loops), is metal ion-specific, involving the coordination of two additional equivalents of K^+, presumably to sites between the G-quartets and nearby loop domains (Fig. 1*C*). As a result of the above-mentioned ion selectivity, we have shown that, in the presence of Li^+ ions only, the folding process can be stopped at the first step (folded with open loops). In the presence of millimolar K^+ ions, folding is driven to the second, more compact form.

In the study presented here, we have validated the above two-step folding model in two ways. We have coupled two-dimensional NMR parameters and molecular modeling to generate a high resolution structure for both the open form of T30695 (Li^+ form) and the closed form of T30695 (the K^+ form). In general, the two high resolution structures are in agreement with the low resolution models derived from optical, thermodynamic, kinetic and one-dimensional NMR data. Specifically, the high resolution model for the Li^+ form of T30695 (Fig. 4) reveals a central pair of G-quartets flanked by extended, disordered loop domains. The model for the K^+ form displays more regularity within the G-quartets, plus flattening and ordering of the adjacent loop domains (Figs. 6 and 7).

In the NMR-constrained structure for the K^+ form of T30695, we have included three bound K^+ ion equivalents, as is required by previous measurements of ion binding stoichiometry (11, 12). In the model (Figs. 6 and 7), we have found that these three K^+ equivalents can be positioned between G-quartets or between G-quartet regions and adjacent loop domains while retaining appropriate K^+ coordination distances. The high resolution structure predicts a nearly planar arrangement of loop base planes, with significant internal, bifurcated H bonding between G and T bases. An orientation of loop thymine bases places the methyl group in a solvent-facing orientation (Fig. 1*E*). Carbonyl groups of the loop G bases are found to be positioned similarly to that seen in a G-tetrad and are found to be in direct association with K^+ ion (Fig. 7).

IC_{50} values of T30695 reveal a strong inhibition of HIV-1 integrase in the K^+-form structure and a poor ability to inhibit HIV activity in the Li^+-form structure (Fig. 8). As seen in Figs. 4 and 7, the Li^+-form structure of T30695 is an asymmetric, less stable G-quartet structure with twisted G-quartet plates and opened loops. These unfolded loops occupy a large space. Compared with Li^+-form structure, K^+ binding to loops induces a structural rearrangement, and the K^+-form structure of T30695 becomes very symmetric and compact. The entire structure closely resembles a perfect cylinder with about 15 Å width and length. Several important features of the K^+-form structure should be noted. There is very little groove structure on the solvent-free surfaces of the K^+ form, and its two ends are nearly planar and identical. The base planes of all G and T residues in the fold are coordinated with K^+ ions. This coordination largely increases the thermal stability of the structure and greatly reduces the capacity for dimer-wise and higher aggregates. The three unhydrated K^+ ions are bound into the center of the G-quartet structure, thereby creating a cylinder with positive charges inside and negative charges on the surface. Although the structure of the complex between T30695 and HIV-1 integrase is not clear yet, these features of the K^+-form structure could enhance the interaction between T30695 and HIV-1 integrase.

TBA is known to lack orderly loop folding in 10 mM KCl with poor IC_{50} values (Figs. 8 and 9 and see Ref. 14). TBA with two T-T loops and a T-G-T loop forms an intramolecular G-quartet structure with one narrow and one wide saddle-shape groove (13, 14). Compared with the K^+-form structure of T30695, the substitution of T-G loops by T-T loops causes a loss of K^+-binding sites between loops and G-quartets (11), forming an unfolded loop and less stable G-quartet structure. An important observation from this study is that the K^+-induced loop folding of the tetrad-forming oligonucleotides, T30695 and T30177, largely increases their inhibition of HIV-1 integrase activity.

Acknowledgments—We thank Dr. Xiaolian Gao for the opportunity to use the 600-MHz NMR spectrometer at the Department of Chemistry, University of Houston, Houston, TX, which is funded by the W. M. Keck Foundation, and we also thank Dr. Luke Pallansch and Carol Lackman-Smith, the Southern Research Institute, Microbiology Department, for the SPA HIV-1 integrase inhibition assay. The calculation of molecular structure was performed in part using the Keck/IMD (Institute for Molecular Design at University of Houston, Houston, TX) Computer Facilities.

REFERENCES

1. Katz, R. A., and Skalka, A. M. (1994) *Annu. Rev. Biochem.* **63,** 133–173
2. Vink, C., and Plasterk, R. H. A. (1993) *Trends Genet.* **9,** 433–437
3. De Clercq, E. (1995) *J. Med. Chem.* **38,** 2491–2517
4. Mazumder, A., Cooney, D., Agbaria, R., Gupta, M., and Pommier, Y. (1994) *Proc. Natl. Acad. Sci. U. S. A.* **91,** 5771–5775
5. Mazumder, A., Neamati, N., Sommadossi, J.-P., Gossdin, G., Schinazi, R. F., Imbach, J.-L., and Pommier, Y. (1996) *Mol. Pharmacol.* **49,** 621–628
6. Mazumder, A., Gazit, A., Levitzki, A., Nicklaus, M., Yung, J., Kohlhagen, G., and Pommier, Y. (1995) *Biochemistry* **34,** 15111–15122
7. Cushman, M., Golebiewski, W. M., Pommier, Y., Mazumder, A., Reymen, D., De Clercq, E., Graham, L., and Rice, W. G. (1995) *J. Med. Chem.* **38,** 443–452
8. Mouscadet, J.-F., Carteau, S., Goulaouic, H., Subra, F., and Auclair, C. (1994) *J. Biol. Chem.* **269,** 21635–21638
9. Rando, R. F., Ojwang, J., Elbaggari, A., Reyes, G. R., Tinder, R., McGrath, M. S., and Hogan, M. E. (1995) *J. Biol. Chem.* **270,** 1754–1760
10. Mazumder, A., Neamati, N., Ojwang, J. O., Sunder, S., Rando, R. F., and Pommier, Y. (1996) *Biochemistry* **35,** 13762–13771
11. Jing, N., Rando, R. F., Pommier, Y., and Hogan, M. E. (1997) *Biochemistry* **36,** 12498–12505
12. Jing, N., Gao, X., Rando, R. F., and Hogan, M. E. (1997) *J. Biomol. Struct. & Dyn.* **15,** 573–585
13. Wang, K. Y., McCurdy, S., Shea, R. G., Swaminathan, S., and Bolton, P. H. (1993) *Biochemistry* **32,** 1899–1904
14. Schultze, P., Macaya, R. F., and Feigan, J. (1994) *J. Mol. Biol.* **235,** 1532–1547
15. Plateau, P., and Gueron, M. (1982) *J. Am. Chem. Soc.* **104,** 7310–7311
16. Piotto, M., Saudek, V., and Sklenar, V. (1992) *J. Biol. Nucleic Magn. Reson.* **2,** 661–665
17. Davis, D. G., and Bax, A. (1985) *J. Am. Chem. Soc.* **107,** 2820–2821
18. Sklenar, V., Miyashiro, H., Zon, G., Miles, H. T., and Bax, A. (1986) *FEBS Lett.* **208,** 94–98
19. Wuthrich, K. (1986) *NMR of Proteins and Nucleic Acids,* pp. 53–60, John Wiley & Sons, Inc., New York
20. Feigon, J., Koshilap, K. M., and Smith, F. W. (1995) *Methods Enzymol.* **261,** 225–255
21. Kang, C., Zhang, X, Ratliff, R., Moyzis, R., and Rich, A. (1992) *Nature* **356,** 126–131